

Combined Ultramicrotomy and Atomic Force Microscopy Study of the Structure of a Bulk Heterojunction in Polymer Solar Cells

A. M. Alekseev^{a, b*}, A. Al-Afeef^c, G. J. Hedley^d, S. S. Kharintsev^e, A. E. Efimov^f,
A. T. Yedrisov^a, N. A. Dyuzhev^b, and I. D. W. Samuel^e

^a National Laboratory Astana, Nazarbayev University, Astana, 010000 Kazakhstan

^b National Research University of Electronic Technology, Moscow, 124498 Russia

^c University of Glasgow, Glasgow, G12 8QQ United Kingdom

^d University of St. Andrews, Scotland, KY16 9AJ United Kingdom

^e Institute of Physics, Kazan Federal University, Kazan, 420111 Russia

^f Federal Research Center for Transplantology and Artificial Organs, Moscow, 123182 Russia

*e-mail: alalus@gmail.com

Submitted February 9, 2017; accepted for publication February 21, 2017

Abstract—A method for visualization via atomic-force microscopy of the internal structure of photoactive layers of polymer solar cells using an ultramicrotome for photoactive layer cutting is proposed and applied. The method creates an opportunity to take advantage of atomic-force microscopy in structural investigations of the bulk of soft samples. Such advantages of atomic-force microscopy include a high contrast and the ability to measure various surface properties at nanometer resolution. Using the proposed method, samples of the photoactive layer of polymer solar cells based on a mixture of PTB7 polythiophene and PC₇₁BM fullerene derivatives are studied. The disclosed details of the bulk structure of this mixture allow us to draw additional conclusions about the effect of morphology on the efficiency of organic solar cells.

DOI: 10.1134/S1063782618010025

1. INTRODUCTION

Solar cells based on organic materials have recently been developed and intensively investigated in laboratories and companies. One of the most promising directions in this field is the development of polymer solar cells (PSCs) with an energy-conversion efficiency of over 10% [1–3]. The attained efficiency of such cells in combination with their simplicity and low cost make them economically attractive. To further increase the efficiency of modern PSCs, it is necessary to have detailed knowledge of the morphology of the photoactive layer, which is a mixture of the organic donor and acceptor forming a bulk heterojunction [4].

The structure of the bulk heterojunction determines a number of very important processes occurring in PSCs, including exciton diffusion and dissociation and charge transport to electrodes.

Among the most widespread methods for studying the nanostructure of photoactive layers are atomic force microscopy (AFM) and transmission electron microscopy (TEM) [5–9]. These two techniques yield complementary information about the sample's nanostructure, since AFM is intended for surface investigations and TEM reveals information about the bulk structure projection. In AFM investigations of the

photoactive-layer structure, a film is usually deposited by centrifuging onto glass coated with indium tin oxide (ITO). An upper electrode and transport layers are not deposited, so the AFM probe has access to the photoactive-film surface. In the TEM measurements, the photoactive layer is transferred from such a sample to a standard TEM measuring lattice. It is extremely important to obtain information on the film structure in the plane perpendicular to the surface, i.e., between electrodes. This is a complex problem to be solved; it requires the use of different surface modification techniques with nanometer spatial resolution. Samples with a photoactive-layer cross section are usually prepared by microtomy or cutting lamellae using a focused ion beam (FIB) [10]. Prepared PSC cross-section samples have predominantly been investigated by high-resolution (as a rule, better than 1 nm) TEM methods, which allow chemical analysis (e.g., energy-filtered transmission electron microscopy (EFTEM)) [11]. In addition, the sample cross sections obtained by cleaving in liquid nitrogen are often studied by scanning electron microscopy, which, as a rule, does not ensure the required resolution. The TEM data obtained on organic samples have poor contrast because of the low atomic number of elements contained in the materials; in addition, the samples are

rapidly destroyed by the electron beam. In contrast to TEM, scanning probe microscopy (SPM) allows one to perform almost nondestructive measurements of organic samples. In addition, the use of different AFM modes yields high contrast on heterogeneous organic samples. Thus, the combination of microtomy and AFM makes it possible to obtain detailed information about the bulk structure of organic samples by measuring different types of interaction between the AFM probe and a sample containing a photoactive-layer cross section. In recent study [12], the combination of microtomy and AFM was used to measure the potential distribution over a PSC cross section. In this study, we use a similar approach, but with other, higher-resolution AFM techniques for studying more topical materials. We study samples of a photoactive film based on a polythiophene derivative commonly abbreviated as PTB7 (Poly({4,8-bis[(2-ethylhexyl)oxy]benzo[1,2-b:4,5-b'] dithiophene-2,6-diyl}{3-fluoro-2-[(2-ethylhexyl) carbonyl] thieno[3,4-b] thiophenediyl})) and an acceptor based on a PC₇₁BM fullerene ([6, 6]-phenyl-C71-butyric acid methyl ester) [13]. Investigations of this mixture added to 3% diiodooctane (DIO) yielded a record-breaking energy-conversion efficiency for a single-layer PSC (9.2%) [14]. This mixture was intensively studied by different methods, so, in general, the structure of this photoactive layer is fairly well-studied [15–19]. However, some problems concerning the bulk heterojunction configuration between electrodes remain unsolved. The aim of this study is to obtain data on the bulk nanostructure of PTB7 polymer-based photoactive layers. The photoactive-layer cross sections prepared by microtomy are studied using AFM techniques. The complementary method used is high-angle annular dark-field scanning transmission electron microscopy (HAADF STEM). As was shown in several studies, this method used for studying organic composites allows the TEM contrast to be significantly improved [11, 20, 21]. Comparison of the data obtained by ultramicrotomy and AFM in combination with FIB TEM show no serious damage or strain in the photoactive layer upon microtomy and reveal good correlation of the results obtained using the two techniques. At the same time, TEM does not reveal some structural details that can be easily seen on SPM images. The importance of the results obtained is confirmed by recent studies of the PTB7 modification, which allows an even higher energy conversion efficiency to be attained [3, 22].

2. EXPERIMENTAL

Samples for microtomy were fabricated using polyethylene-terephthalate (PET) substrates with a poly(3,4-ethylenedioxythiophene) poly(styrenesulfonate) (PEDOT:PSS) (Clevios AI4083) hole transport layer and a PTB7:PC₇₁BM photoactive layer deposited by conventional centrifuging techniques.

The PTB7:PC₇₁BM solution in chlorobenzene was prepared in a concentration of 25 mg/mL at a mass ratio of 1 : 1.5. Before centrifuging, the solution was mixed for 5 h at a temperature of 50°C. The mixture was deposited in a glove box in a nitrogen atmosphere at a speed of rotation of 1000 revolutions per minute. When using the solution with 3 vol. % of DIO, the samples after film deposition were placed in vacuum (in a chamber with a residual pressure of 10⁻⁵ mbar) to remove the remaining DIO. The sample was coated with a CYTOP amorphous fluoropolymer (AGC Chemicals Europe) with a thickness of several micrometers. Thus, the obtained sample contained a photoactive layer suitable for forming a cross section by microtomy. Right before microtomy, the sample was embedded in epoxy resin and a pyramidal blank was preliminarily cut using a glass knife. During microtomy under standard conditions, the cut thickness was 200 nm. Sample slices were cut with a Leica UC6 ultramicrotome under standard conditions. After cutting, the sample cross sections floating on the knife dish surface were deposited onto a thin (0.17 mm) glass slide (Fig. 1a). Thus, the samples for optical and probe microscopy study of the bulk heterojunction structure were prepared. The cut thickness *d* was verified by measuring the surface topography near the cut edge (Fig. 1b). It can be seen that the thickness *d* is consistent with the microtome program settings, although there is some deviation to the smaller side, which can be attributed to the microtomy parameters and mechanical properties of the sample. The cut surface as a whole is smooth (the surface roughness is much smaller than the cut thickness). The pronounced dark lines in Fig. 1a are folds that occur during cut transfer to the glass substrate. Upon AFM scanning of the surface, the regions between the folds were chosen.

We fabricated samples of two types: with photoactive layers of PTB7:PC₇₁BM and PTB7:PC₇₁BM with 3% of DIO added (hereinafter referred to as PTB7:PC₇₁BM:DIO). During deposition of the photoactive layer onto the PET substrate, a thin intermediate centrifuged PEDOT:PSS sublayer was used to keep the photoactive-layer structure the same as that of the reference samples on the glass/ITO substrate.

The photoactive layers for TEM investigations were deposited onto a standard glass/ITO substrate coated with the centrifuged PEDOT:PSS layer [11]. The thickness of the film with DIO deposited onto PET was larger than when using a standard substrate with ITO.

The SPM measurements were performed using an Integra Aura facility (NT-MDT) with NSG01 and CSG10 probes (NT-MDT). The phase contrast was measured in the tapping mode with repulsion forces being dominant.

The lamella with a photoactive-layer cross section for TEM study was prepared using a NovaNanolab 100 double-beam system, which is comprised of a scan-

ning electron microscope and a FIB. A lamella $10 \times 4 \times 80 \mu\text{m}$ in size was cut perpendicular to the sample surface and contained all of the layers. The TEM measurements were performed using an ARM (JEOL) microscope.

The spectra of giant Raman scattering enhanced by a plasmon nanoantenna were detected using an INTEGRA Spectra measuring system (NT-MDT). For this purpose, we used an inverted optical scheme and SPM configuration with measurements of the lateral forces on the basis of a quartz resonator with an attached gold nanoantenna. The conical optical nanoantenna was formed by the adaptive electrochemical etching of gold wire in a solution of hydrochloric acid (37%) and ethanol (96%) in the volume ratio of 1 : 1 [23, 24]. In the measurements, we used a laser with a radiation wavelength of 532 nm.

3. RESULTS AND DISCUSSION

The prepared samples containing sections of PTB7:PC₇₁BM and PTB7:PC₇₁BM:DIO photoactive layers deposited onto glass substrates were studied by probe microscopy techniques to establish the bulk structure of the photoactive layers. Previously, the structure of such films was investigated by probe and electron microscopy, as well as X-ray diffractometry [11, 15–19]; however, a number of problems concerning the bulk structure of the heterojunction remained unsolved. In particular, as was emphasized in recent publication [11], the details of the film structure in the plane perpendicular to the electrodes are still unclear. This is important for understanding the operation of modern high-efficiency organic solar cells, since the interelectrode structure directly affects charge transport. To investigate this, we prepared samples with photoactive-layer cross sections using the above-described microtomy-based method. To study the cross section of the PTB7:PC₇₁BM structure (Fig. 1a), we used topography measurements in the tapping mode and the phase-contrast technique. As was mentioned above, the use of AFM for studying the photoactive-layer cross section and spatial arrangement of the heterojunction has a number of advantages over other techniques (e.g., electron microscopy) since this method ensures high contrast at a rather high spatial resolution. The phase measurement mode of the oscillating probe allows one to determine the component distribution in the mixture, since the phase depends on different properties of the surface. The change in the phase ϕ upon contact between the oscillating probe and the surface is related to the energy loss $\sin\phi \propto E_{\text{dis}}$, where E_{dis} is the probe energy loss for the oscillation period [25]. Thus, the measured phase contrast is determined by surface properties leading to energy loss, i.e., by adhesion, friction, viscoelasticity, etc. In general, it is impossible to unambiguously establish a contrast source in the phase image due to the complexity and diversity of factors

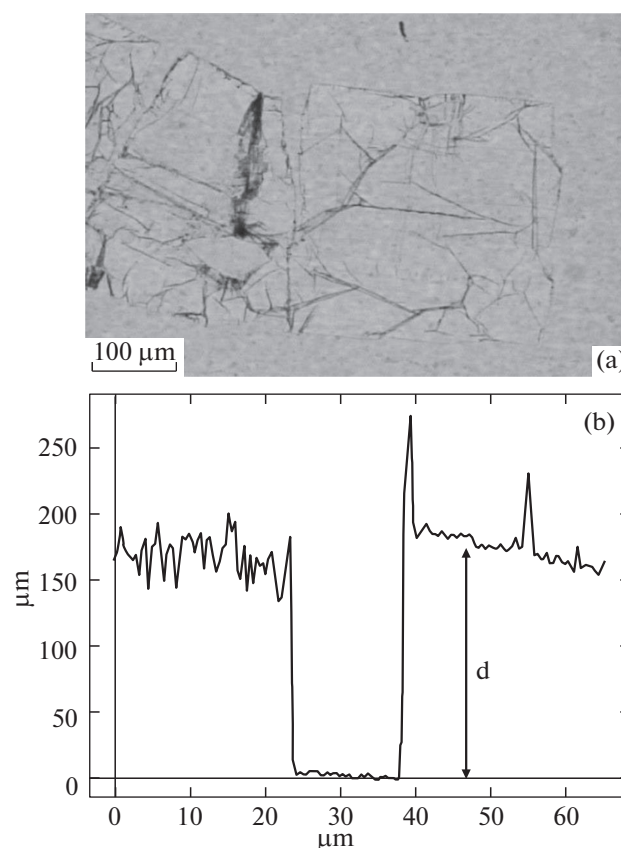


Fig. 1. (a) Optical image of the sample cut on glass and (b) AFM profile of the cut on glass.

leading to the phase shift. The method under consideration, however, is commonly accepted in studying polymer samples using scanning electron microscopes and allows one to distinguish components with different properties in the mixtures at a resolution of ~ 1 nm.

The results of structural measurements of the photoactive-layer cross section for the rather well-studied PTB7:PC₇₁BM mixture without any additions are presented in Fig. 2a, where one can clearly see the photoactive layer between the white dashed lines. Figures 2a–2c show domains with an approximately elliptical shape, which were previously investigated by TEM [11]. Using the HAADF STEM technique, we measured also a single elliptical domain in the film cross section formed by cutting a thin lamella with the FIB (Fig. 3). One can see inhomogeneities with diffuse contours inside the elliptical domain in Fig. 3, which prevent unambiguous conclusions about the internal domain structure from being made. The contrast in the phase image (Fig. 2c) appeared much better pronounced and allowed the internal structure of the mixture to be determined. The internal domain structure can be clearly seen and demonstrates that the domain contains both the donor and acceptor distributed nonuniformly. As was established previously, the domains consist mainly of PC₇₁BM [11, 18, 19]; there-

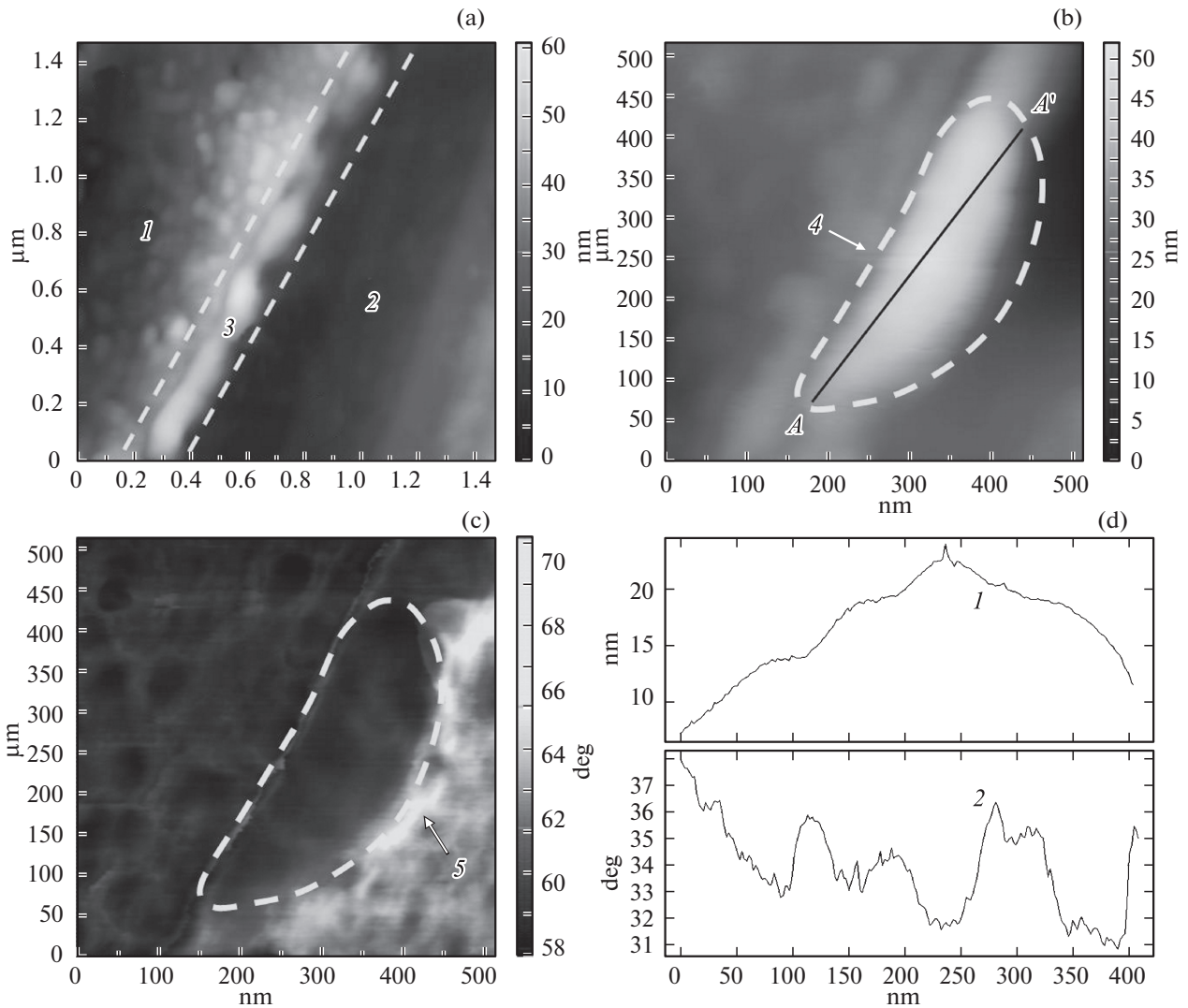


Fig. 2. AFM images of the PTB7:PC₇₁BM film cross section: (a, b) surface texture and (c) phase contrast. Images in (b) and (c) show the same region. (1) PET, (2) CYPOT, (3) PTB7:PC₇₁BM layer, (4) PEDOT, and (5) the layer enriched with PTB7. (d) Texture (1) and probe oscillation phase (2) in the AA' cross section (see (b)).

fore, the light stripes in the elliptical domain (Fig. 2c, on the right) can be interpreted as polymer-enriched regions. In our settings of the tapping measurement mode with the dominant repulsion forces, the light areas correspond to a softer material leading to a larger energy loss (polymer). Figure 2d shows the texture and phase image of the same region. It can be seen that the phase of oscillations of the probe cantilever changes in the places with smooth texture; i.e., the phase contrast reflects specifically different compositions in the domain. The lack of correlation between the texture and phase contrast is one piece of evidence showing the sensitivity of the measured phase to the surface composition. Thus, the domain structure represents regions several tens of nanometers in size enriched with the fullerene and separated by areas with significant PTB7 polymer content. The distribution of inho-

mogeneities over the domain thickness and their shape and size in the film cross section are demonstrated for the first time. In addition, the phase image (Fig. 2c) contains a pronounced polymer-enriched thin layer coating the elliptical domain. It is the bright area adjacent to the dotted line on the right (designated by 5).

Thus, the combination of microtomy and probe-microscopy measurements of the sample cross section yields valuable data on the nanostructure of the photoactive layer, which are generally confirmed by electron-microscopy data. Such an approach is complementary to the more widespread FIB and TEM cross-section measurements and allows the advantages of SPM to be applied. The established domain structure features make it possible, in particular, to explain the fairly high energy-conversion efficiency of solar cells



Fig. 3. HAADF STEM image of the elliptical domain in the PTB7:PC₇₁BM photoactive layer cross section.

based on this mixture (6.2% [13]); specifically, the nonuniform domain structure increases the bulk heterojunction area, which leads to an increase in the number of excitons dissociating with the formation of free charge carriers. In addition, Fig. 2c is indicative of the possible existence of a continuous path for holes in the domain bulk through polymer stripes, which facilitates charge transport to the electrode. At the same time, the presence of a polymer-enriched thin film coating the domains can reduce the efficiency of a solar cell due to limited electron transport to the electrode.

The second sample studied by us contains the PTB7:PC₇₁BM:DIO layer cross section. The structure was studied using the following probe microscopy techniques: topography measurements in the tapping mode, phase contrast, friction force microscopy, and HAADF STEM. The importance of investigations of this sample is based, in particular, on the assumption concerning the separation of the donor and acceptor in the bulk of the photoactive layer at which the polymer concentration near the centrifuged mixture surface increases. This assumption is based on the fact that the maximum efficiency (9.2%) is attained using the inverted architecture [14]. Then, enrichment of the surface with the polymer can also activate charge transport to the electrodes, since the PTB7 polymer is characterized by hole conductivity.

To prove that the sample prepared by us contains the section of the film under study, we analyzed the chemical composition of the surface cut via the microscopy of giant Raman scattering enhanced by the AFM probe [26, 27]. As was shown in [23, 24], the optical resolution of this technique on polymer samples is 50–60 nm. The signal measured by us corresponds to the spectral region of 1515–1570 cm⁻¹, within which the spectral maxima of both the polymer and fullerene are located. The giant Raman scattering data obtained on the sample surface clearly reveal the areas containing PTB7 and PC₇₁BM, which confirms the presence of a photoactive film in the prepared sample (Fig. 4).

Figure 5a shows the surface topography of the PTB7:PC₇₁BM:DIO photoactive layer cut measured by the SPM in the tapping mode. The photoactive layer is located between the two dashed lines. Some topography variations on the cut surface can be attributed, first of all, to knife defects and nonuniform

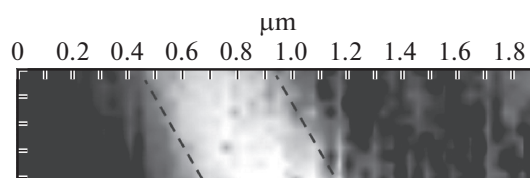


Fig. 4. Giant Raman spectra from the sample cross section with the PTB7:PC₇₁BM:DIO film. Dashed lines show the PTB7:PC₇₁BM:DIO layer boundaries.

mechanical properties of the cut surface. The structure consisting of strips with a period of ~150 nm perpendicular to the photoactive layer results from vibrations during cutting. Figures 5b and 5c show the cut surface topography and phase contrast for the same region of the PTB7:PC₇₁BM:DIO photoactive layer.

It was most important to determine the degree of homogeneity of the photoactive layer in the bulk of PTB7:PC₇₁BM:DIO. It follows from Fig. 5c that the properties of the photoactive layer that lead to variations in the AFM probe oscillation phase are uniform over the layer thickness. The phase contrast only shows the effect of topography; no features or inclusions in the bulk of the film were observed. If the polymer concentration varied, the phase contrast inside the photoactive layer would be nonuniform. Thus, the AFM data indicate that the properties of the film in the bulk of the sample are homogeneous. To confirm this result, we used friction-force microscopy in the contact mode. In this technique, the lateral probe bending caused by friction forces is measured. In the contact probes used in the experiment, the force of interaction with the surface estimated from the dependence of the cantilever deviation on coordinate *Z* of the scanner was < 10 nN. Such a weak interaction force allowed the polymer surface to be investigated with the minimum destruction in the contact mode. Figure 5d shows the friction-force distribution over the PTB7:PC₇₁BM:DIO photoactive-layer cross section. Again, the results obtained show that the friction-force distribution over the layer thickness is uniform and, consequently, the donor and acceptor are uniformly mixed, at least, accurate to the resolution of the technique used (several nanometers). The contrast in Fig. 5d repeats the features observed in the surface image (Fig. 5b); no traces of phase separation or domain formation are observed. The surface pattern affects the oscillation phase of the cantilever and its lateral bending; however, the presence of regions with different properties would be reflected as contrast unrelated to the texture.

To confirm the conclusion about the film structure, the sample with the PTB7:PC₇₁BM:DIO section was studied by HAADF STEM. The results of measurements and layer identification in the sample cross section are illustrated in Fig. 6. Slight contrast varia-

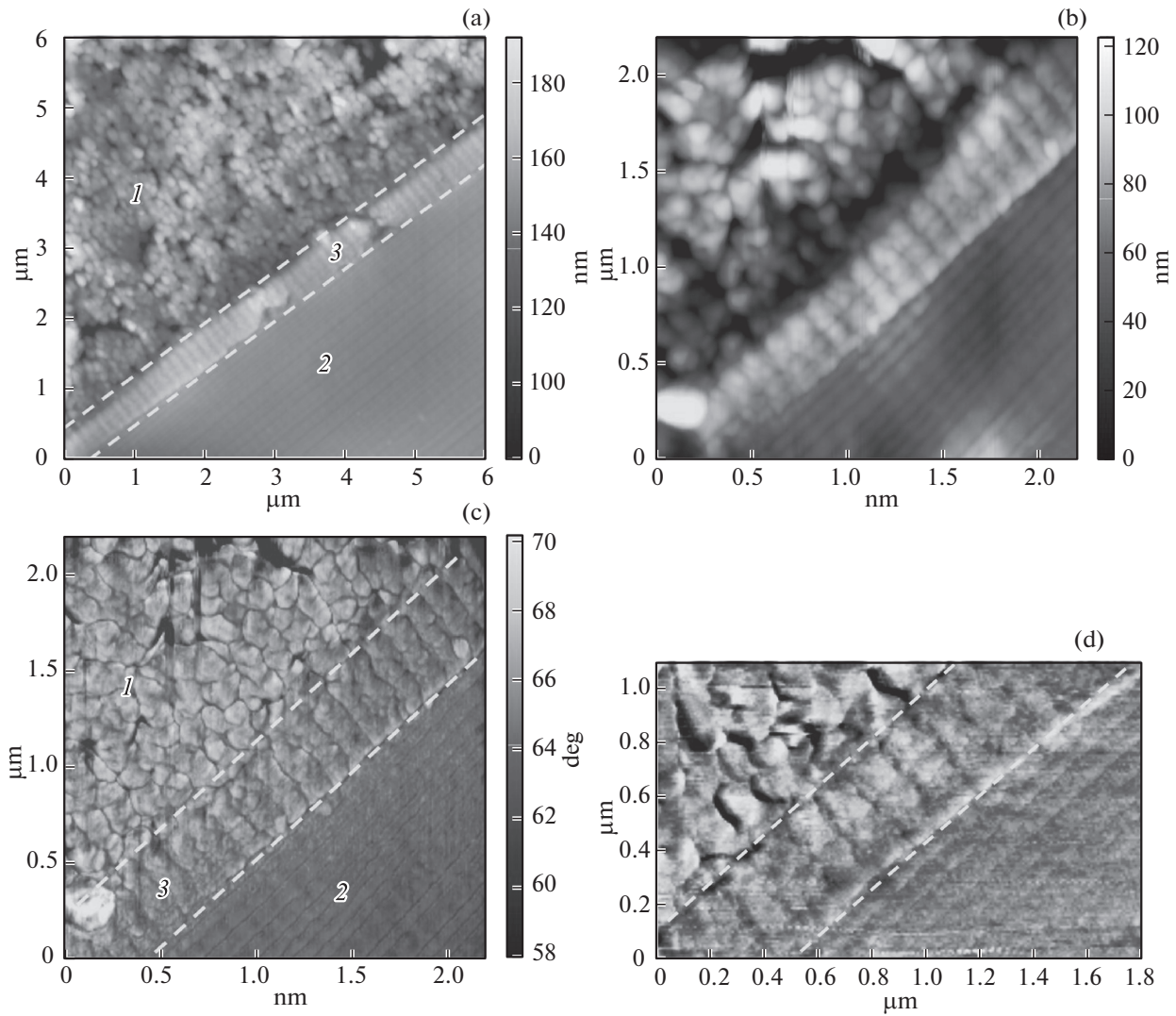


Fig. 5. AFM images of the PTB7:PC₇₁BM:DIO cuts: (a, b) topography, (c) phase contrast, and (d) friction-force distribution. Images in (b) and (c) show the same region. The photoactive layer is located between dashed lines. (1) CYPOT, (2) PET, and (3) PTB7:PC₇₁BM:DIO layer.

tions in the photoactive layers do not allow us to draw a conclusion about the presence of phase separation or the formation of agglomerates in the film. This result

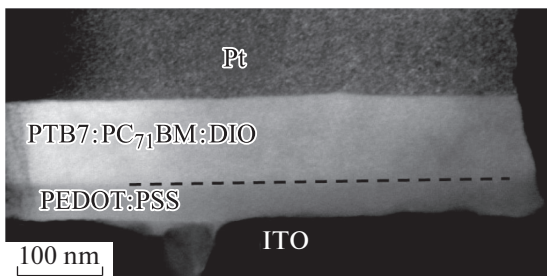


Fig. 6. HAADF STEM image of the PTB7:PC₇₁BM:DIO sample cross section.

is consistent with conclusions based on the AFM data. Thus, the data obtained by the high-resolution probe microscopy and HAADF STEM techniques are indicative of the high degree of component intermixing in the PTB7:PC₇₁BM:DIO film and of the absence of noticeable inhomogeneities in the bulk of the film on the nanometer scale. This conclusion is important for understanding the operation of cells based on PTB7:PC₇₁BM with a 3-% DIO addition, which showed a record-breaking, until recently, energy conversion efficiency of single-layer PSCs (9.2%).

Thus, the above assumption about separation of the polymer and fullerene in the bulk of the PTB7:PC₇₁BM:DIO photoactive layer, where the surface is enriched with the polymer, was not confirmed by our results. The fact that the inverted configuration

of a solar cell led to the maximum efficiency for the investigated donor and acceptor needs further explanation and investigations. Further development of this technique requires improvement in the microtomy modes to obtain higher-quality cuts. In particular, it seems promising to perform microtomy upon sample cooling in liquid nitrogen.

4. CONCLUSIONS

In this study, we proposed and applied a method for studying the internal structure of organic solar cells, which is based on microtomy and probe microscopy. The approach used allowed us to establish the details of the fullerene-enriched domain structure in the PTB7:PC₇₁BM photoactive layer. Comparison of the results obtained with TEM data makes it possible to conclude that our approach is promising for investigations of structural components and determination of the local properties of the bulk of organic material mixtures with nanometer resolution. The results obtained for the PTB7:PC₇₁BM:DIO mixture by different probe microscopy methods showed a high degree of component intermixing in the bulk of the mixture and the absence of phase segregation on the nanometer scale.

ACKNOWLEDGMENTS

This study was supported by the Ministry of Education and Science of the Republic of Kazakhstan, Program NU-Berkli 0115RK03029) and the Ministry of Education and Science of the Russian Federation, state task no. 14.578.21.0188 (unique agreement identifier RFMEFI57816X0188).

S.S. Kharintsev thanks the Russian Foundation for Basic Research, project no. 15-42-02339 for support. A. Al-Afeef thanks the Lord Kelvin/Adam Smith Foundation for support.

We are grateful to D.A. MacLaren and I. MacLaren (University of Glasgow) for help in forming the HAADF STEM images.

A part of the studies was carried out using equipment of the Shared Service Center "MST and EKB".

REFERENCES

1. W. Zhao, D. Qian, S. Zhang, S. Li, O. Inganäs, F. Gao, and J. Hou, *Adv. Mater.* **28**, 4734 (2016).
2. S. Zhang, L. Ye, and J. Hou, *Adv. Energy Mater.* **6**, P1502529 (2016).
3. Q. Wan, X. Guo, Z. Wang, W. Li, B. Guo, W. Ma, M. Zhang, and Y. Li, *Adv. Funct. Mater.* **26**, 6635 (2016).
4. C. J. Brabec, N. S. Saricifci, and J. C. Hummelen, *Adv. Funct. Mater.* **11**, 15 (2001).
5. X. Yang, J. Loos, S. C. Veenstra, W. J. H. Verhees, M. M. Wienk, J. M. Kroon, M. A. J. Michels, and R. A. J. Janssen, *Nano Lett.* **5**, 579 (2005).
6. S. D. Oosterhout, M. M. Wienk, S. S. van Bavel, R. Thiedmann, L. J. A. Koster, J. Gilot, J. Loos, V. Schmidt, and R. A. J. Janssen, *Nat. Mater.* **8**, 818 (2009).
7. M. J. M. Wirix, P. H. H. Bomans, M. M. R. M. Hendrix, H. Friedrich, N. A. J. M. Sommerdijk, and G. de With, *J. Mater. Chem. A* **3**, 5031 (2015).
8. A. Alexeev, J. Loos, and M. M. Koetse, *Ultramicroscopy* **106**, 191 (2006).
9. D. C. Coffey, O. G. Reid, D. B. Rodovsky, G. P. Bartholomew, and D. S. Ginger, *Nano Lett.* **7**, 738 (2007).
10. J. Loos, J. K. J. van Duren, F. Morrissey, and R. A. J. Janssen, *Polymer* **43**, 7493 (2002).
11. A. Alekseev, G. J. Hedley, A. Al-Afeef, O. A. Ageev, and I. D. W. Samuel, *J. Mater. Chem. A* **3**, 8706 (2015).
12. M. Scherer, R. Saive, D. Daume, M. Kröger, and W. Kowalsky, *AIP Adv.* **3**, 092134 (2013).
13. Y. Liang, Z. Xu, J. Xia, S. T. Tsai, Y. Wu, G. Li, C. Ray, and L. Yu, *Adv. Mater.* **22**, E135 (2010).
14. Z. He, C. Zhong, S. Su, M. Xu, H. Wu, and Y. Cao, *Nat. Photon.* **6**, 591 (2012).
15. S. J. Lou, J. M. Szarko, T. Xu, L. Yu, T. J. Marks, and L. X. Chen, *J. Am. Chem. Soc.* **133**, 20661 (2011).
16. M. R. Hammond, R. J. Kline, A. A. Herzing, L. J. Richter, D. S. Germack, H.-W. Ro, C. L. Soles, D. A. Fischer, T. Xu, L. Yu, M. F. Toney, and D. M. DeLongchamp, *ACS Nano* **5**, 8248 (2011).
17. B. A. Collins, Z. Li, J. R. Tumbleston, E. Gann, C. R. McNeill, and H. Ade, *Adv. Energy Mater.* **3**, 65 (2012).
18. F. Liu, W. Zhao, J. R. Tumbleston, C. Wang, Y. Gu, D. Wang, A. L. Briseno, H. Ade, and T. P. Russell, *Adv. Energy Mater.* **4**, 1676 (2014).
19. G. J. Hedley, A. J. Ward, A. Alekseev, C. T. Howells, E. R. Martins, L. A. Serrano, G. Cooke, A. Ruseckas, and I. D. W. Samuel, *Nat. Commun.* **4**, 2867 (2013).
20. J. Loos, E. Sourty, K. Lu, G. de With, and S. van Bavel, *Macromolecules* **42**, 7 (2009).
21. E. Sourty, S. van Bavel, K. Lu, R. Guerra, G. Bar, and J. Loos, *Microsc. Microanal.* **15**, 251 (2009).
22. Z. He, B. Xiao, F. Liu, H. Wu, Y. Yang, S. Xiao, C. Wang, T. P. Russell, and Y. Cao, *Nat. Photon.* **9**, 174 (2015).
23. S. Kharintsev, A. Alekseev, V. Vasilchenko, A. Khari-tonov, and M. Salakhov, *Opt. Mater. Express* **5**, 2225 (2015).
24. S. Kharintsev, A. Alekseev, and J. Loos, *Spectrochim. Acta A* **171**, 139 (2017).
25. J. P. Cleveland, B. Anczykowski, A. E. Schmid, and V. B. Elings, *Appl. Phys. Lett.* **72**, 2613 (1998).
26. L. Novotny and B. Hecht, *Principles of Nano-Optics* (Cambridge Univ. Press, New York, 2012).
27. P. Verma, T. Ichimura, T. Yano, Y. Saito, and S. Kawata, *Laser Photon. Rev.* **4**, 548 (2010).

SPELL: OK

Translated by E. Bondareva